JOURNAL OF MATERIALS SCIENCE: MATERIALS IN MEDICINE 9 (1998) 337–345

In vitro investigation of novel calcium phosphates using osteogenic cultures

C. KNABE, W. OSTAPOWICZ, R. J. RADLANSKI*
*Department of Restorative Dentistry and Periodontology, and *Department of Oral Biology, University Hospital Benjamin Franklin, Free University of Berlin, Aßmannshauser Strasse 4-6, 14197 Berlin, Germany*

R. GILDENHAAR, G. BERGER
Federal Institute for Material Research and Testing, Laboratory of Biomaterials, Unter den Eichen 87, 12200 Berlin, Germany

R. FITZNER, U. GROSS‡
Institute of Clinical Chemistry and Biochemistry, and ‡Institute of Pathology, University Hospital Benjamin Franklin, Free University of Berlin, Hindenburgdamm 30, 12200 Berlin, Germany

A rat bone marrow stromal cell (RBM) culture was used to evaluate novel bioactive calcium phosphate ceramics. Three rapidly resorbable, glassy crystalline materials with the main crystalline phase $Ca_2KNa(PO_4)_2$ were investigated (sample code GB 1a, GB 14, GB 9). These materials were designed to exhibit a higher degree of biodegradability than tricalcium phosphate. Additionally, a bioactive glass ceramic of low biodegradability was examined (sample code AP 40). RBM cells were cultured on the disc-shaped test substrata for 14 d. The culture medium was changed and calcium and phosphate concentrations of the medium were determined daily. Specimens were evaluated using light microscopy and morphometry of the cell-covered substrate surface, scanning electron microscopy and energy dispersive X-ray analysis. Except for GB 1a, the rat bone marrow cells attached and grew on all substrate surfaces. Of the different calcium phosphate ceramics tested, AP 40 facilitated osteoblast growth and the elaboration of the extracellular matrix to the highest degree followed by GB 9 and GB 14. The inhibition of cell growth encountered with GB 1a seemed to be related to its high phosphate ion release.

1. Introduction

The current gold standard for bone reconstruction in craniomaxillofacial applications is the autogenous bone graft. Recently, the concept of guided bone regeneration (GBR) has become a widely accepted mode of treatment in implant dentistry. Localized ridge augmentation prior to the placement of dental implants is one of the clinical indications for GBR. At present, autogenous bone grafts combined with barrier membranes are used to support the membrane as a space-maintaining device in cases of extensive bone defects [1]. Using biodegradable bone substitutes as a membrane-supporting device would simplify GBR, since second-site surgery for harvesting autografts could be avoided, thus reducing morbidity associated with bone harvesting. Bioactive calcium phosphate ceramics are among the alloplastic materials suitable for bone regeneration. The substances most commonly applied and investigated are synthetic or coralline hydroxyapatite (HA) and β-tricalcium phosphate (β-TCP) [2–4]. More recently, bioactive glass ceramic particulates have been used either alone or together with autogenous bone where augmentation is required to reconstruct osseous defects [5–9]. All of these materials are known to be biocompatible and osteoconductive and are categorized as bioactive materials [10], because new bone can bond to the ceramic surface. These materials differ considerably in several aspects, one of which being the rate of resorption. HA resorbs very slowly compared to β-TCP [11, 12]. Even with β-TCP, biodegradation has been reported to be incomplete 40 months after grafting in human periodontal intrabony defects [13]. Particularly in non-load-bearing applications such as alveolar ridge augmentation, dental implant placement should be preceeded by the use of an optimal synthetic bone substitute as a scaffold for bone formation. This substance must be rapidly absorbable to permit new bone growth without residual particles that may interfere with preparation of the implant bed at implant surgery.

Therefore, novel rapidly resorbable, glassy crystalline materials have been developed which exhibit stable crystalline $Ca_2KNa(PO_4)_2$ phases and can be

0957–4530

synthesized with a wide composition range and varying degrees of solubility. These materials have a higher solubility than tricalcium phosphates (TCP) [14] and thus are designed to exhibit a higher degree of biodegradability.

In vitro model systems using osteogenic cell cultures have become invaluable tools for the initial assessment of biological reactions to candidate implant materials [15, 16]. In this context, *in vitro* models serve a dual purpose. Used for initial biological evaluation and screening of novel biomaterials, they reduce the number of *in vivo* studies.This is particularly appealing when creating a novel material with a wide composition range. Secondly, *in vitro* experiments offer the advantage of a completely defined environment for studying cell–substrate interactions enabling visualization of cell behaviour on the electron microscopic level [17]. Because most bone replacement materials are implanted in adult bone and they directly contact bone marrow tissue, it is advantageous to use a rat bone marrow stromal cell culture system, in which both bone cell and bone tissue interfaces can be established *in vitro*, resulting in an interfacial morphology similar to that reported in *in vivo* experiments [16, 18].

The present study is part of a series of investigations aimed at the development of a standardized *in vitro* test system for evaluating novel bioactive calcium phosphate ceramics of varying composition.

2. Experimental procedure

2.1. Materials

We investigated three novel, rapidly resorbable, glassy crystalline materials based on calcium alkaline orthophosphates (sample code GB series) designed to exhibit a higher degree of biodegradability than TCP and a glass ceramic of low biodegradability. The compositions (wt %) of the calcium phosphate ceramics examined are listed in Table I.

The main crystalline phase of the GB materials consisted of a newly synthesized chemical with the formula $Ca_2KNa(PO_4)_2$ [19]. By adding magnesia and silica to the pseudobinary system $CaKPO_4$–$CaNaPO_4$ glassy crystalline materials can be created with a wide composition range. Directly after melting, these materials crystallize spontaneously during cooling and contain both crystalline and glassy phases. All of the GB samples examined were sintered materials with the crystalline phase $Ca_2KNa(PO_4)_2$. Additionally, GB 14 samples displayed a small amorphous portion containing magenesium-potassium phosphate. GB 9 samples exhibited a small amorphous portion of silica phosphate. GB 1a samples had a large amount of amorphous and crystalline phases containing magnesium-potassium phosphate. Preparation of these materials has been described in detail elsewhere [14, 20]. GB 9 samples have previously been referred to as GB 9/1 [20]. The bioactive glass-ceramic (sample code AP 40) was based on crystalline phases of apatite and wollastonite.

For the GB 14, GB 9 and GB 1a specimens, disc-shaped pellets were prepared from powder (grain size smaller than 40 μm) by a pressing process and subsequently sintered. This procedure produced discs 9 mm diameter and 2 mm thick (surface roughness 10 μm). AP 40 specimens were prepared by sectioning discs from cast cylinders (15 mm diameter, surface roughness 10 μm). The cut surface was subsequently temperature treated. The surface morphology of the specimens is illustrated by the scanning electron micrographs presented in Fig. 1. Thermanox® cell culture coverslips (15 mm diameter, Nunc Inc.) served as controls. The ceramic specimens were sterilized at 300 °C for 3 h. Phase transformations do not occur below 600 °C.

2.2. Cell isolation and cultures

Primary rat bone-marrow cells (RBM) were explanted using the method described by Maniatopoulos *et al.* [21] and Davies *et al.* [15]. Briefly, the femoral epiphysis was removed from young adult Wistar rats, and the marrow was then washed out using supplemented tissue culture medium. RBM cells were cultured in alpha-Minimal Essential Medium (Gibco, Paisley, UK) containing 15% foetal calf serum, antibiotics (0.1 mg/ml penicillin G, 50 μg/ml gentamicin, 0.3 μg/ml amphotericin B) and supplemented with 10^{-8} M dexamethasone, 50 μg/ml ascorbic acid and 10 mM β-glycerophosphate (Sigma, St Louis, MO, USA) at 37 °C, in a humidified, 5% CO_2/95% air incubator. After 5 d primary culture, cells were detached using trypsin and seeded at a density of 3×10^4 cells cm^{-2} on the test substrata on 24-well plates (Becton Dickinson, Franklin Lakes, NJ, USA). GB 14, GB 9 and GB 1a specimens had been preincubated in 500 μl fully supplemented medium for 24 h prior to cell seeding and the 24 h wash was then discarded. The culture medium was changed daily. The osteoblastic nature of the RBM cells was confirmed by alkaline phosphatase cytochemistry.

TABLE I Compositions of calcium phosphate ceramics examined

Material	Composition (wt%)							
	CaO	P_2O_5	Na_2O	K_2O	MgO	SiO_2	TCP	CaF_2
GB 14	30.67	43.14	9.42	14.32	2.45			
GB 9	32.25	40.81	8.91	13.54	2.57	1.92		
GB 1a	20.70	42.90	11.60	17.30	7.50			
AP 40	16–19		3–5	0.1–0.3		42–45	23–25	3.0–5.5

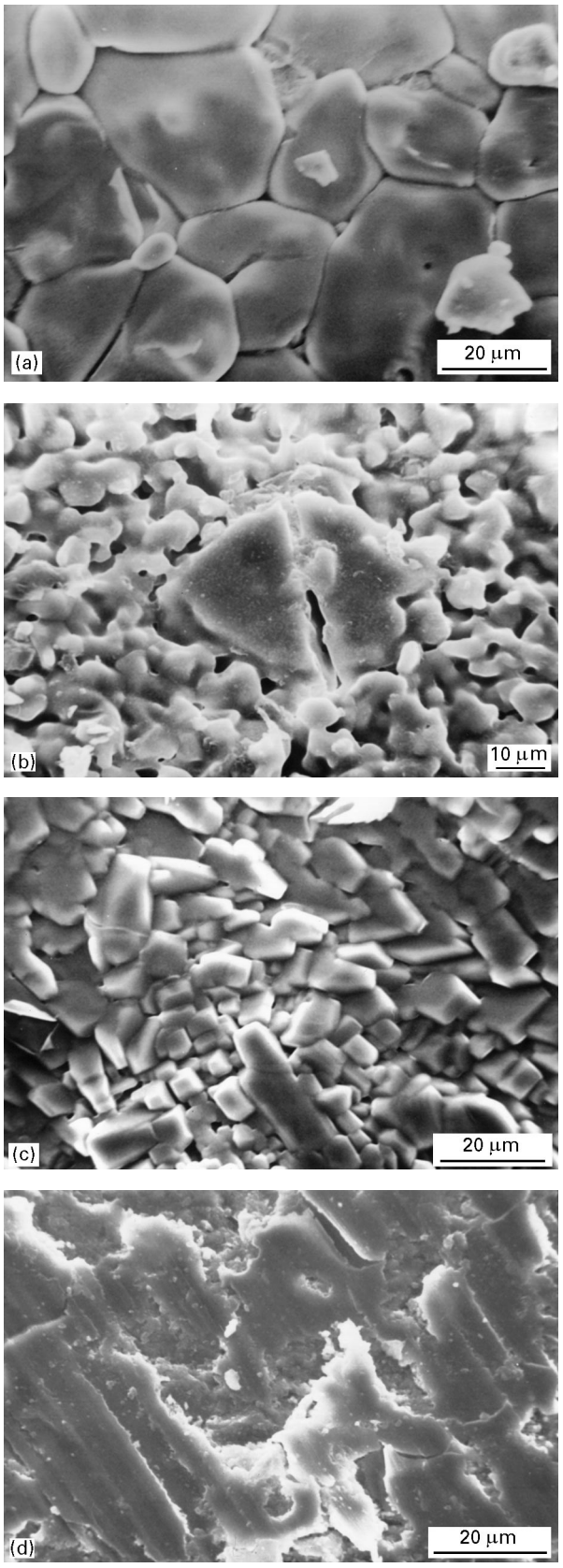

Figure 1 Scanning electron micrographs of the calcium phosphates examined: (a) GB 14, (b) GB 9, (c) GB 1a, (d) AP 40.

2.3. Light microscopy and histomorphometry

After 14 d incubation, cell cultures were briefly rinsed twice in phosphate-buffered saline (PBS) solution, pH 7.2 and fixed in methanol for 20 min. The specimens were then washed with distilled water and air-dried. This was followed by application of Giemsa staining solution. For morphometric evaluation, eight samples of each material were tested in each experiment which were run in triplicate. The cell-covered surface was morphometrically determined using a Leitz Orthoplan microscope equipped with a personal Computer (PC 32-05 IBM-Siemens, MS-DOS), a video camera (Phillips LDK 12), a cursor and a graphic tablet (Matrox MVP-AT). A grading system was applied which divided cell density into the following four classes. Class I consisted of areas with solitary cells, cell debris or no cells (Fig. 2) and thus were not considered cell-covered substrate surfaces. Class II represented reticular, loosely arranged cell formations (Fig. 3), and class III a dense cell layer (Fig. 4). Class

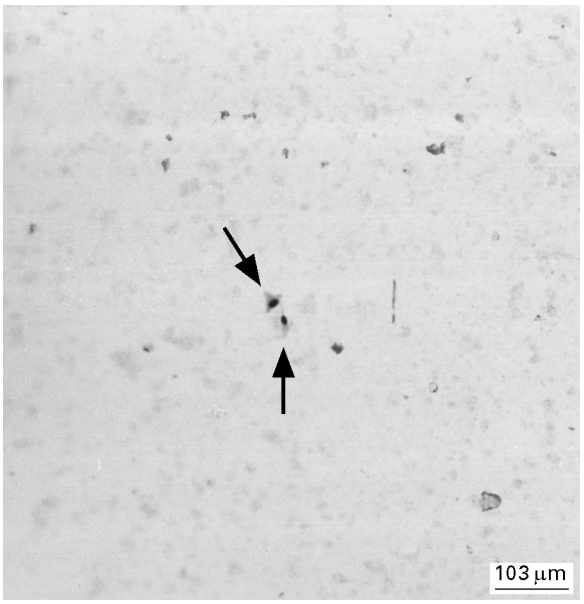

Figure 2 Light micrograph of class I cell coverage: solitary cells (arrows), cellular debris or no cells.

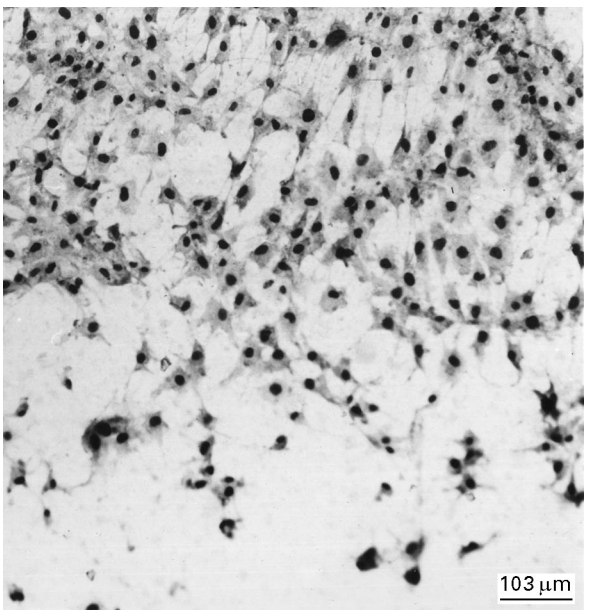

Figure 3 Light micrograph of class II cell coverage: reticular loosely arranged cell formations.

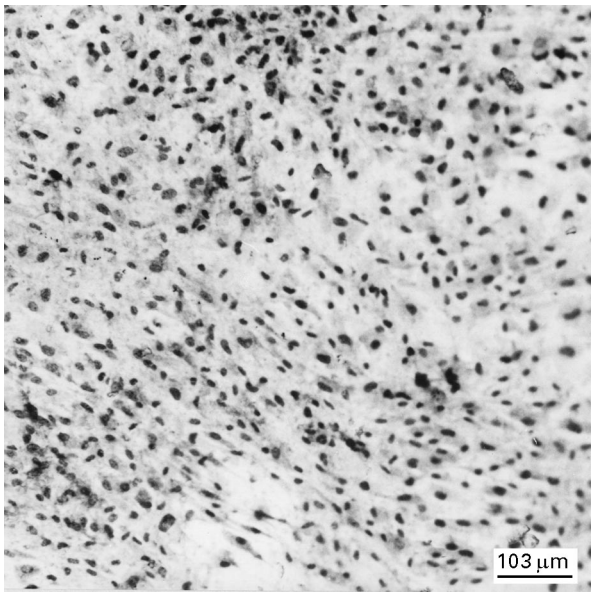

Figure 4 Light micrograph of class III cell coverage: a dense cell layer.

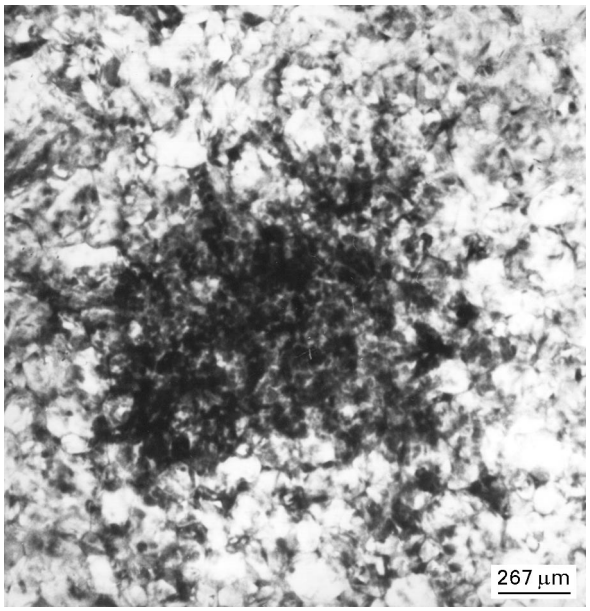

Figure 5 Light micrograph of class IV cell coverage: a nodular area with increased cell density and multilayers.

IV was used for nodular areas with increased cell density and multilayers (Fig. 5). Values for Thermanox and AP 40 were adjusted for the larger surface area of the specimens by dividing by 2.78 (Thermanox and AP 40 specimens had a diameter of 15 mm and a surface area of 176.7 mm^2, whereas the remaining specimens had a diameter of 9 mm with a surface area of 63.6 mm^2). Box-and-Whiskers-Plots (smallest values, lower tenth, lower fourth, median, upper fourth, upper tenth, largest values) were used for graphic illustration. Statistical analysis of the cell-covered substrate surface was performed by testing the differences between the substrata using the Kruskal–Wallis test with a level of significance of $p < 0.05$. To compare the different test substrata to each other, multiple testing was performed using the Mann–Whitney U test with a level of significance of $p < 0.05$, which included applying the Bonferroni-adjustment according to the number of tests performed.

2.4. Scanning electron microscopy

Additional specimens were prepared for scanning electron microscopy (SEM) and energy dispersive X-ray (EDX) analysis after 14 d incubation. SEM and EDX analysis of the different substrate surfaces were performed after fabrication and after the 14 d incubation period. Specimens of each test material incubated for 14 d without cells served as controls. Preparation for SEM and EDX analysis included rinsing the cells cultured on the different substrata three times in 0.1 M cacodylate-buffered solution, pH 7.2 and fixing in 3% glutaraldehyde in 0.1 M sodium cacodylate-buffered solution at 4 °C for 15 min. This was followed by washing with cacodylate buffer 0.1 M, pH 7.2 three times and dehydration once in 30%, 50%, 70%, 80%, 90% and 96% ethanol, and three times in absolute ethanol for 10 min each. The specimens were then washed three times in hexamethyldisilazane (HMDS) for 10 min each and air-dried for 24 h. The dried specimens were glued on to aluminium stubs, sputter-coated with gold and examined in a Phillips SEM 505 at an accelerating voltage of up to 20 kV. A Roentec® energy dispersive X-ray microanalyser attached to a Cambridge Stereoscan 150 MK2 SEM was utilized for EDX analysis.

2.5. Measurement of calcium and phosphate concentrations in the culture medium

Calcium and phosphate concentrations of the culture medium from the different substrata were retrieved after the 24 h preincubation period and daily throughout the incubation period. They were determined by atomic absorption spectrometry (AAS) and photometric analysis. A BM/Hitachi 704 spectrometer was used for the photometric analysis.

3. Results

3.1. Morphometry

The results of the morphometric evaluation of the cell-covered substrate surface are demonstrated in Figs 6 and 7. Fig. 7 shows the size of surface areas according to class II, III and IV cell coverage for each material tested.

After 14 d incubation, calcium phosphate ceramic GB 1a displayed only a few solitary cells and cell debris. Statistical analysis of the cell-covered substrate surface yielded statistically significant differences in the test substrata ($p < 0.001$, Kruskal–Wallis test). The substrate surface was almost completely covered by cells with AP 40, GB 9 (Fig. 8) and Thermanox, while the cells on GB 14 specimens covered a considerably smaller percentage of the surface area (Fig. 6). A mean of 99.1% of the surface area was covered by cells on AP 40, 97.8% (mean) on GB 9 and

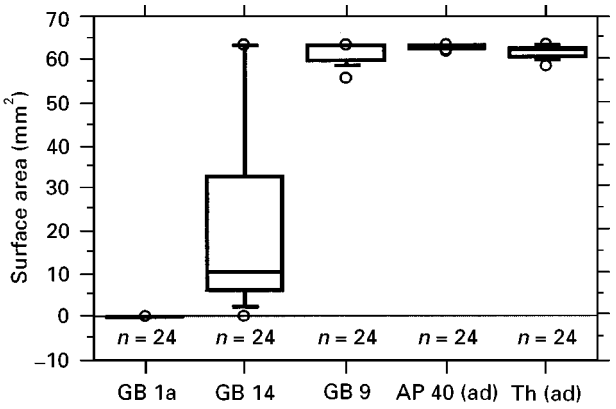

Figure 6 Box-and-Whiskers plot of the morphometric results of the cell-covered substrate area for the different test substrata. (AP 40 (ad), Th (ad): AP 40 and Thermanox-adjusted values with respect to the larger surface area of Thermanox and AP 40 as compared to the other specimens).

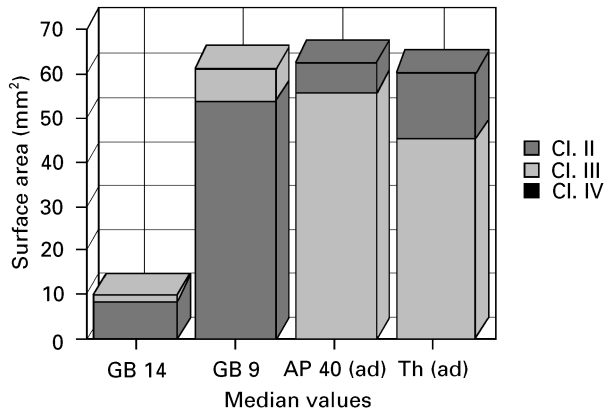

Figure 7 Histogram of class II, III and IV distribution (median values of substrate surface areas with class II, III and IV cell coverage).

97.4% (mean) on Thermanox. There was a statistically significant difference between AP 40 and Thermanox ($p = 0.0007$, Mann–Whitney U test) but not between AP 40 and GB 9 or GB 9 and Thermanox. Compared to GB 14, the difference in the cell-covered substrate area was statistically significant for AP 40, GB 9 and Thermanox ($p < 0.0001$, Mann–Whitney U test). Values for GB 14 showed the widest scattering range (Fig. 6). Among the different ceramics tested, AP 40 displayed the highest cell density, and, similar to Thermanox, class III and IV cell coverage predominated (Fig. 7). With GB 9 and GB 14, the cell-covered substrate surface was graded mainly as class II, but also as class III to a lesser degree (Fig. 7). Although the difference between cell-covered substrate areas of AP 40 (adjusted values) and GB 9 was not statistically significant, class III and IV surface areas were significantly larger with AP 40 ($p < 0.0001$, Mann–Whitney U test). The same was true for the comparison of class III and class IV areas of Thermanox (adjusted values) and GB 9 ($p < 0.0001$, Mann–Whitney U test). Moreover, Thermanox specimens exhibited a significantly larger area of class IV cell coverage than AP 40 (Fig. 7) ($p < 0.0001$, Mann–Whitney U test).

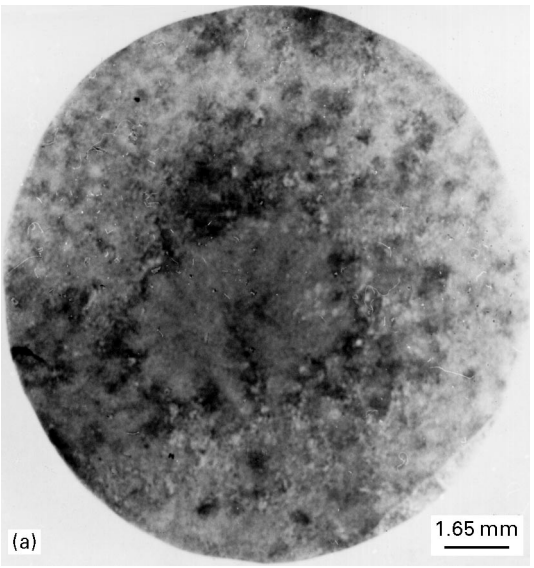

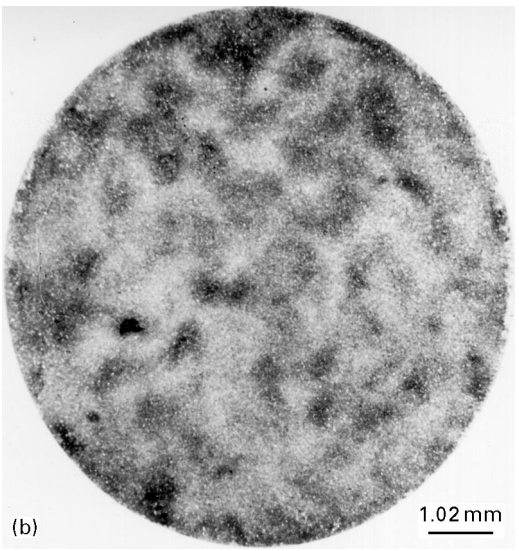

Figure 8 Photograph of (a) AP 40, Giemsa, and (b) GB 9 specimens, Giemsa, showing that the substrate surface is almost completely covered by cells. Areas of increased cell density can already be detected on the macroscopic level.

3.2. EDX analysis and calcium and phosphate concentrations in the culture medium

Fig. 9 lists the calcium and phosphate concentrations in the culture medium and the corresponding pH values for the different calcium phosphates measured after 24 h preincubation and daily throughout the 14 d incubation period.

SEM and EDX analysis of the GB 1a substrate surface revealed phosphorus- and magnesium-rich precipitations and an increase in phosphorus on the ceramic surface after 14 d incubation. Moreover, strongly increased phosphate concentrations were determined in the culture medium. This was associated with a considerable decrease in the calcium concentration (Fig. 9b) and an elevated pH (Fig. 9c).

With GB 9 and GB 14, there was a moderate increase in phosphate concentrations in the medium, while calcium concentrations were moderately decreased. EDX analysis detected phosphorus- and

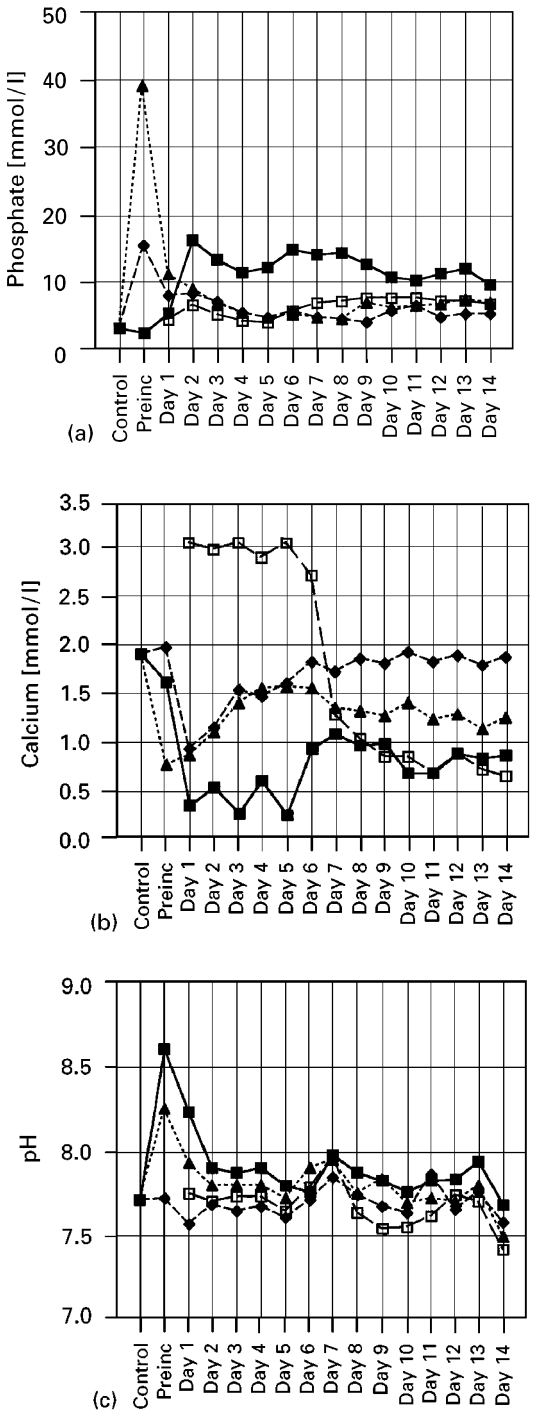

Figure 9 The calcium and phosphate concentration with the corresponding pH in fully supplemented culture medium (control) and culture medium from the different calcium phosphate ceramics retrieved after 24 h preincubation and daily throughout the 14 d incubation period: (a) phosphate concentration, (b) calcium concentration, (c) pH. (■) GB 1a, (◆) GB 14, (▲) GB 9, (□) AP 40.

magnesium-rich precipitations with GB 14. GB 9 specimens did not reveal any significant changes in the composition of the substrate surface. The medium retrieved from AP 40 specimens showed an increased calcium content throughout the first 6 d which decreased towards the end of the experiment; this corresponded to a moderate increase in phosphate levels during the second week. EDX analysis of the ceramic surface detected an increase in phosphorus after 14 d incubation.

3.3. Scanning electron microscopy

After 14 d incubation, a multilayer of RBM cells and elaboration of a multilayered extracellular matrix (ECM) displaying fibrillar components was observed on AP 40, GB 9 and Thermanox (Figs 10–12). The

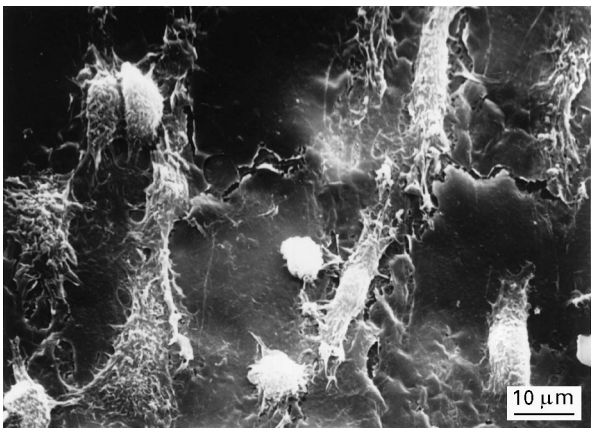

Figure 10 Scanning electron micrograph of GB 9. A multilayer of RBM cells and extracellular matrix cover the GB 9 surface. The drying produced some rupturing of the surface layer.

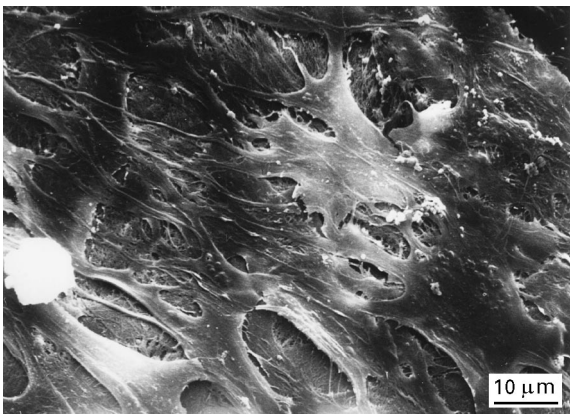

Figure 11 Scanning electron micrograph showing elaboration of a multilayered ECM and a multilayer of RBM cells on AP 40 after 14 d incubation. The drying procedure caused some rupturing of this covering layer. Collagen fibres formed a dense mat.

Figure 12 Scanning electron micrograph showing elaboration of a multilayered ECM and a multilayer of RBM cells on Thermanox after 14 d incubation. The drying procedure caused this matrix to rupture in some areas. Collagen fibres are visible.

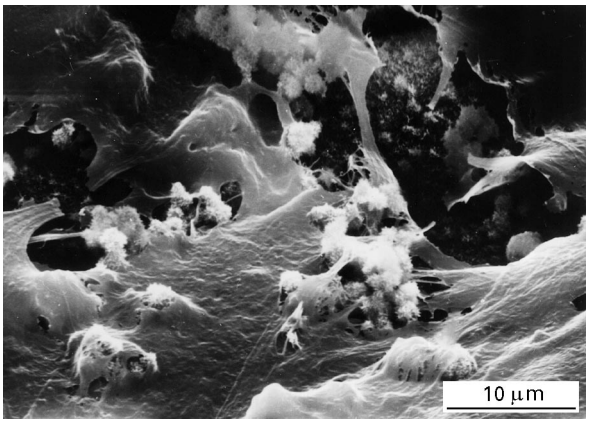

Figure 13 Scanning electron micrograph of GB 14. The substrate surface is partially covered by a dense layer of RBM cells and extracellular matrix. Precipitations are still visible and are partially enclosed.

drying procedure caused this matrix to rupture in some areas. Fibrous material and granular components became visible in some areas. On GB 14 specimens, cell layers and the extracellular matrix seemed to be less dense and stratified, exhibiting fewer fibrillar components (Fig. 13).

4. Discussion

Our investigations demonstrate that significant differences with respect to cell growth and proliferation were observed between the different substrata. Except for GB 1a, rat bone marrow cells attached and grew on all substrate surfaces. The inhibitory effect on cell growth observed with GB 1a was associated with considerably increased phosphate and decreased calcium concentrations in the culture medium, corresponding to an increase in pH. In addition, extensive phosphorus- and magnesium-rich precipitations were observed. Among the calcium phosphates examined, AP 40 and GB 9 displayed the largest percentage of cell-covered substrate surface. AP 40 specimens exhibited a considerably higher degree of cell density similar to that of the Thermanox controls. GB 14 specimens facilitated osteoblast growth to a lesser degree with values for the cell-covered substrate surface having the widest scattering range. Moreover, extracellular matrix (ECM) elaboration was observed. EDX analysis demonstrated matrix mineralization on the Thermanox specimens. EDX analysis of ECM on AP 40 and GB 9 yielded spectra similar to those of the Thermanox control specimens, demonstrating major peaks for calcium and phosphorus. Owing to the detection level of the EDX microanalyser, however, it cannot be reliably excluded that peak generation was influenced by the underlying ceramic substrata. These findings suggest that the matrix observed on AP 40 and GB 9 may also have been mineralized. However, a more sensitive method will have to be applied to definitely confirm this hypothesis. A suitable assay may be tetracycline labelling of the mineralized matrix produced in culture as proposed by Lowenberg *et al.* [22] and Todescan *et al.* [23]. On GB 14, ECM elaboration seemed to be less developed than on the other substrata.

Furthermore, when using an *in vitro* rat bone marrow culture system capable of mineralized matrix production, examinations for the presence of specific non-collagenous bone proteins [24] seem to be of interest for evaluating implant materials. Ozawa and Kasugai [25] demonstrated osteopontin and bone sialoprotein expression in rat bone marrow stromal cell cultures on hydroxyapatite, glass ceramics and titanium using cell cultures prepared accordingly. Therefore, analysis of these matrix proteins will be of interest for further studies with the calcium phosphate ceramics presented here.

In general, cell–biomaterial interactions are influenced by substratum properties such as surface texture, surface chemistry, surface free energy and surface charge [26–31]. Moreover, in connection with resorbable bioactive calcium phosphate ceramics, adequate solubility behaviour in biological fluids is a prerequisite for biodegradability. Thus ion release from these materials also influences cell–substratum interactions, because especially divalent cations are known to be active in cell adhesion mechanisms [32]. It also has been suggested that the surface transformation of bioactive ceramics into a biologically equivalent apatite, i.e. carbonated hydroxyapatite, is associated with the phenomenon of bioactivity [33–38]. Immersion studies in *Tris*-HCl buffer solution or protein-free simulated body fluids have been proposed as the first qualitative test for bioactivity [36, 39]. However, investigations pertaining to the effect of serum proteins on solution-induced surface transformations of bioactive ceramics have indicated that these surface reactions were retarded or impeded with several of the ceramics tested in the presence of serum proteins [40]. These surface reactions are another factor influencing the cell response to bioactive calcium phosphates ceramics.

The results of our study indicate that the inhibitory effect on cell growth encountered with GB 1a seems to be related to its high phosphate ion release. Data from a previous study in which the solution kinetics of GB 14, GB 9 and GB 1a in 0.2 M *Tris*-HCl buffer solution were determined with a circulating reactor [20] also showed a high solubility and phosphate ion release for GB 1a. Regarding the elution behaviour of GB 14 and GB 9 samples, the solubility of phosphate ions and potassium was higher for GB 14 than GB 9, while GB 9 exhibited higher calcium solubility [14]. The analysis of calcium and phosphate concentrations in the culture medium did not show these differences. However, phosphorus- and magnesium-rich precipitations were detected by EDX analysis of GB 14 samples, which may be indicative of a phosphate ion release. Cytotoxicity tests on AP 40 and GB 14 extracts showed these materials to be non-toxic [41]. Based on our data, the factors accounting for the cell growth differences observed between AP 40, GB 14 and GB 9 cannot be clearly distinguished, especially whether these differences are merely related to varying solubility or to the presence of magnesium- or silica-containing additives. Ion release from these materials, however, seems to be an important parameter, because enhanced cell growth was found in previous

investigations on various rapid resorbable calcium phosphate ceramics, in which the culture medium was changed daily instead of every 2–3 d [42, 43]. Therefore, cultures were also refed daily in our study. The role of magnesium ion release and magnesium content in precipitations from GB 1a and GB 14 will have to be further examined with regard to diminished cell growth on these substrata.

Previous experiments on differently modified AP 40 specimens showed that samples with temperature-treated surfaces had significantly enhanced cell growth compared to untreated specimens. However, EDX analysis and electron probe microanalysis (EPMA) of the substrate surface did not reveal any significant differences accounting for these observations (unpublished data). It may be speculated that solution-induced surface transformation phenomena after immersion in a tissue culture medium might be related to these observations because, in a previous study, apatite formation was detected on AP 40 by Auger infrared reflection spectroscopy after immersion in aqueous solution [44].

Consequently, further investigations will have to be performed to clarify the underlying mechanisms of the phenomena observed in our study, particularly the role of ion levels on cell adhesion, metabolic cell activity and surface reactions at the ceramic surface. Future studies should determine magnesium, potassium and silicate ion concentrations in the culture medium as well as the calcium and phosphate contents. Moreover, the development of a standardized *in vitro* test for bioactive rapidly resorbable calcium phosphates could imply that ion levels in the culture medium may have to be adjusted for solubility kinetics of different materials. In cell cultures, relatively small fluid volumes are used, while *in vivo* removal of eluted ions by metabolic or circulatory processes may prevent excessively elevated ion levels at the cell biomaterial interface.

5. Conclusion

It is found that the inhibition of cell growth on GB 1a seemed to be related to its very high phosphate ion release. The other three biomaterials facilitated osteoblast growth and ECM elaboration, AP 40 to the highest degree followed by GB 9 and GB 14. Further investigations are required to determine the role of ion levels in the culture medium and of solution-induced surface transformations on cellular adhesion, metabolism and proliferation, and to thus clarify the underlying mechanisms of the phenomena reported here.

Acknowledgements

The authors thank Mrs B. Scheidereiter and Mrs A. Schoenknecht for their technical assistance with the EDX and AAS analyses.

References

1. D. BUSER, K. DULA, H.-P. HIRT and H. BERTHOLD, in "Guided Bone Regeneration in Implant Dentistry", edited by D. Buser, C. Dahlin and R. K. Schenk, (Quintessence, Chicago, 1994) p. 189.
2. R. Z. LE GEROS, in "Hydroxyapatite and Related Materials", edited by P. W. Brown and B. Constanz, (CRC Press, Boca Raton, 1994) p. 3.
3. V. SHETTY and T. J. HAN, *Dent. Clin. North Am.* **35** (1991) 521.
4. M. J. YASZEMSKI, R. G. PAYNE, W. C. HAYES, R. LANGER and A. C. MIKOS, *Biomaterials* **17** (1996) 175.
5. J. WILSON, A. E. CLARK, E. DOUEK, J. KRIEGER, W. KING SMITH and J. SAVILLE ZAMET, in "Bioceramics 7", edited by Ö. H. Andersson, R.-P. Happonen and A. Yli-Urpo, (Butterworth-Heinemann, Oxford, 1994) p. 453.
6. J. WILSON, A. E. CLARK, M. HALL and L. HENCH, *J. Oral Impl.* **4** (1993) 295.
7. J. WILSON and S. LOW, *J. Appl. Biomater.* **3** (1992) 123.
8. J. WILSON, L. YU and B. BEALE, in "Bioceramics 5", edited by T. Yamamuro, T. Kokubo and T. Nakamura, (Butterworth-Heinemann, Oxford, 1992) p. 139.
9. E. J. G. SCHEPERS and P. PINRUETHAI, in "Bioceramics 6", edited by P. Ducheyne and D. Christiansen, (Butterworth-Heinemann, Oxford, 1993) p. 113.
10. L. L. HENCH, *Ann. NY Acad. Sci.* **523** (1988) 54.
11. R. E. HOLMES, R. W. BUCHOLZ and V. MOONEY, *J. Orthop. Res.* **5** (1987) 114.
12. P. S. EGGLI, W. MULLER and R. K. SCHENK, *Clin. Orthop. Rel. Res.* **232** (1988) 127.
13. J. F. SAFFAR, M. L. COLOMBIER and R. DETIENVILLE, *J. Periodontol.* **61** (1990) 209.
14. G. BERGER, R. GILDENHAAR and U. PLOSKA, *Biomaterials* **16** (1995) 1241.
15. J. E. DAVIES, B. LOWENBERG and A. SHIGA, *J. Biomed. Mater. Res.* **24** (1990) 1289.
16. B. LOWENBERG, R. CHERNECKY, A. SHIGA and J. E. DAVIES, *Cells Mater.* **1** (1991) 177.
17. J. E. G. HULSHOFF, K. VAN DIJK, J. P. C. M. VAN DER WAERDEN, J. G. C. WOLKE, L. A. GINSEL and J. A. JANSEN, *J. Biomed. Mater. Res.* **29** (1995) 967.
18. J. E. DAVIES, R. CHERNECKY, B. LOWENBERG and A. SHIGA, *Cells Mater.* **1** (1991) 3.
19. M. SCHNEIDER, R. GILDENHAAR and G. BERGER, *Cryst. Res. Technol.* **29** (1994) 671.
20. G. BERGER, R. GILDENHAAR and U. PLOSKA, in "Bioceramics 8", edited by J. Wilson, L. L. Hench and D. C. Greenspan, (Butterworth-Heinemann, Oxford, 1995) p. 453.
21. C. MANIATOPOULOS, J. SODEK and A. H. MELCHER, *Cell. Tiss. Res.* **254** (1988) 317.
22. B. F. LOWENBERG, R. TODESCAN, A. SHIGA, R. YAKUBOVIC, S. GLOVER, P. GIRARD and J. E. DAVIES, in "Transactions of the 5th World Biomaterials Congress", edited by D. C. Smith (University of Toronto Press, Toronto 1996) p. 668.
23. R. TODESCAN, B. F. LOWENBERG, M. M. HOSSEINI and J. E. DAVIES, *ibid*., p. 721.
24. J. SODEK, Q. ZHANG, H. A. GOLDBERG, C. DOMENICUCCI, S. KASUGAI, J. L. WRANA, H. SHAPIRO and J. CHEN, in "The Bone-Biomaterial Interface", edited by J. E. Davies, (University of Toronto Press, Toronto, 1991) p. 97.
25. S. OZAWA and S. KASUGAI, *Biomaterials* **17** (1996) 23.
26. D. M. BRUNETTE, *Int. J. Oral Maxillofac. Implants* **3** (1988) 231.
27. D. M. BRUNETTE, J. RATKAY and B. CHEHROUDI, in "The Bone-Biomaterial Interface", edited by J. E. Davies, (University of Toronto Press, Toronto, 1991) p. 170.
28. R. M. SHELTON, A. C. RASMUSSEN and J. E. DAVIES, *Biomaterials* **9** (1988) 24.
29. K. GOMI and J. E. DAVIES, *J. Biomed. Mater. Res.* **27** (1993) 429.
30. A. F. VON RECUM and T. G. VAN KOOTEN, *J. Biomater. Sci. Polymer Edn* **7** (1995) 181.
31. K. E. HEALEY, C. H. THOMAS, A. REZANIA, J. E. KIM, P. J. MCKEOWN, B. LOM and P. E. HOCKBERGER, *Biomaterials* **17** (1996) 195.
32. R. U. HYNES, *Cell* **69** (1992) 11.

33. G. DACULSI, R. Z. LE GEROS, E. NERY, K. LYNCH and B. KEREBEL, *J. Biomed. Mater. Res.* **23** (1989) 883.
34. L. L. HENCH, *J. Am. Ceram. Soc.* **74** (1992) 1487.
35. P. DUCHEYNE and J. CUCKLER, *Clin. Orthop.* **276** (1992) 102.
36. T. KOKUBO, in "Bone-Bonding Materials", edited by P. Ducheyne, T. Kokubo and C. A. van Blitterswijk, (Reed Health Care Communications, The Netherlands, 1993) p. 31.
37. S. RADIN and P. DUCHEYNE, *J. Biomed. Mater. Res.* **27** (1993) 35.
38. *Idem*, *ibid.* **28** (1994) 1303.
39. O. H. ANDERSSON, K.VÄHÄTALO, A. YLI-URPO, R.-P. HAPPONEN and K. H. KARLSSON, in "Bioceramics 7", edited by Ö. H. Andersson, R.-P. Happonen and A. Yli-Urpo, (Butterworth-Heinemann, Oxford, 1994) p. 67.
40. S. RADIN and P. DUCHEYNE, *J. Biomed. Mater. Res.* **39** (1996) 273.
41. H.-U. PICKER, H. ARPS, ST. KÖHLER and G. BERGER, *Z. Zahnärzt Implantol.* **9** (1993) 11.
42. C. KNABE, R. GILDENHAAR, G. BERGER, W. OSTAPOWICZ, R. FITZNER, R. RADLANSKI, U. GROSS and G. K. SIEBERT, in "Transactions of the 21st Annual Meeting of the Society for Biomaterials", edited by P. M. Portner, (Society for Biomaterials, Minneapols 1995) p. 156.
43. C. KNABE, R. GILDENHAAR, G. BERGER, W. OSTAPOWICZ, R. FITZNER, R. RADLANSKI, U. GROSS and G. K. SIEBERT,*Int. J. Artif. Organs* **18** (1995) 432.
44. G. BERGER and M. GIEHLER, *Phys. Status Solidi* (*a*) **86** (1984) 531.

Received 26 February
and accepted 5 September 1997